Enhanced Photocatalytic Activity of Two Dimensional SrTiO$_3$ Nano Structures for Dye Degradation

Y. Allssa
  Shahid Beheshti University

S. T. Sajjadian
  Shahid Beheshti University

S. M. Hamidi (✉ m_hamidi@sbu.ac.ir)
  Laser and Plasma Reseaarch Institute   https://orcid.org/0000-0002-5298-2224

S. Sadeghi
  Shahid Beheshti University

M. R. Nabid
  Shahid Beheshti University

Research Article

Abstract

The combination of the properties of nanostructures, photocatalytic semiconductors, and plasmonic materials can significantly contribute to improving the performance of the entire photocatalysis process. We tried to produce a unique catalyst by combining these three properties. We have produced a two-dimensional nanostructure which was then coated with gold as a plasmonic material followed by $SrTiO_3$ as semiconductor material. The result was the production of the first catalyst of its kind made in this way, which offered notable results. The degradation ability of the sample was examined with different degrees of pH of rhodamine B dye, where we achieved the highest degradation, 16%, at pH10.

Introduction

Semiconductor photocatalysis has attracted a lot of interest decomposition of pollution, green energy and also water purification [1], [2]. However, semiconductors suffer from a high rate of recombination between electrons and holes, and as a result, low quantum yield [3]. To overcome this drawback, nanostructures are considered, due to their high surface to volume ratio, lower electron-hole recombination rate, and more active sites for catalysis process in comparison with the bulk semiconductors [4], [5]. Among these semiconductors, titanate perovskites, $ATiO_3$ (A = Ca, Sr, Ba, etc.), have a large band gap and important photocatalytic properties [6]. Titanate perovskites are considered to be promising materials in the photocatalytic processes due to their high physicochemical stability and their resistance to photo-corrosion [7][8].

$SrTiO_3$ (STO) is an excellent candidate in this category as an n-type semiconductor with a large indirect energy gap due to its crystal structure and morphology [9]. This wide band gap is categorized into two indirect and direct band gaps as; indirect one of 3.25 eV, which is similar to anatase structure with TiO_2, located between the upper valence band, which mainly composed of O2p, besides the empty states Ti3d (t2g). The other one is direct band gap at 3.75 eV [10], located between O2p and Ti3d (eg) levels [9]. Figure 1 displays the scheme of the direct and indirect of STO band gaps.

According to this band gap, $SrTiO_3$ is a superior photocatalyst but unfortunately only under UV light, which contains nearly 5% of sunlight [6][11]. Thus, $SrTiO_3$ must be adapted to enhance its absorptivity in the visible light region. One method involves deposition of noble metals (Au, Ag and Pt) on the surface of semiconductor [12][13]. Unfortunately, use of these rare or precious nano metals can reduce the separation time of photo generated charge carriers thereby decreasing the photocatalytic efficiency.

Tao XIAN et al. prepared Au-$SrTiO_3$ nanocomposites using a photocatalytic reduction method by which the Au nanoparticles with particle size of 726nm were deposited on the surface of $SrTiO_3$ particles with an average diameter of 55 nm. Au-$SrTiO_3$ exhibited improved simulated sunlight photocatalytic activity compared to its visible light photocatalytic activity [14]. Lei Ma et al. observed photocatalytic activities of $SrTiO_3$ in the ultraviolet and visible regions by surface plasmon enhancement, after incorporating Ag nanoparticles on STO surfaces. They proposed a two-step excitation model for surface plasmon -

enhanced photocatalysis in $SrTiO_3$ [15]. Xiangchao Ma et al. proved that oxygen vacancies induce various and important effects on the properties of materials. They investigated the thermodynamic stabilities and electronic properties of oxygen vacancies on the $SrTiO_3$ (001) surface and at the Au/ $SrTiO_3$ (001) interface systematically [16]. Dilara Saadetnejad and Ramazan Yildirim tested the visible light water splitting activity of Au-Al/$SrTiO_3$. They prepared Al/$SrTiO_3$ by solid state reaction, while Au loading was done via homogenous deposition precipitation method. The UV-vis analysis revealed that Al doping enhanced the band energy of $SrTiO_3$ [17]. A. K. Wahab et al. investigated the hydrogen production from ethanol as a bio-fuel over 0.5 wt% Rh/$SrTiO_3$ and 0.5 wt% Pt/$SrTiO_3$ perovskite materials. The found that the rate of photo-catalytic reaction of ethanol to hydrogen was far higher on Pt/$SrTiO_3$ compared to Rh/$SrTiO_3$ [18]. Ag – $SrTiO_3$ nanocomposites synthesized via one-pot solvothermal method was used to induce a broad plasmonic resonance absorption in the visible light range in comparison with pristine $SrTiO_3$. Their work provided a facile and controllable route to prepared Ag – $SrTiO_3$ plasmonic nanocomposite photocatalyst featuring excellent visible light activities and selectivity for NO abatement [19]. Yanfei Fan et al. prepared $SrTiO_3$ with surface oxygen vacancies via carbon reduction under a high temperature. They applied it successfully as a photocatalyst water splitter to produce clean hydrogen energy under visible light irradiation without any sacrificial reagent for the first time [20].

In the noble metal- photocatalysts structures, noble metal nanoparticles can act as a trap for photo-induced electrons, thereby preventing the recombination process of photogenerated charge carriers [21]. More importantly, these metal nanoparticles can absorb a specific range of visible light, thereby inducing the surface plasmon resonance (SPR) effect [22] [21]. Upon the excitation of SPR, the generated hot electrons in the noble metal nanoparticles are directly injected into the CB of the attached photocatalysts [23][24]. The remaining hot electrons and holes in the noble metal nanoparticles can take part in the photocatalytic reaction, making photocatalysts have visible light photocatalytic activity [25] [26]. In addition, SPR can improve the local electric field of neighboring semiconductors, leading to increased electron-hole separation rate [23][24]. Gold (Au) with its own interband transition and surface plasmon resonance can play a significant role in visible light photocatalysis activities [17]; Au-decorated $SrTiO_3$ was found to exhibit improved visible light photocatalytic activity in water splitting, plus iso-propanol and NO decomposition, and syngas production [13][27].

As mentioned above, use of nanostructure forms in semiconductor layer as well as metallic SPR usage can help us enhance photocatalyst activity. Thus, we proposed two-dimensional structured $SrTiO_3$ as a photocatalyst semiconductor for the first time and after evaluation of its efficiency, we use gold layer's surface lattice resonance to adjust the degradation percentage.

Experimental Procedure

The proposed structure is composed of a perforated Polydimethylsiloxane (PDMS) substrate and layer of semiconductor material such as $SrTiO_3$, coated via pulse laser deposition (PLD) method, and a thin layer of gold in order to explore the plasmonic effect on the photocatalytic performance for $SrTiO_3$. To this aim,

0.2 gr of PDMS and 0.02 gr of hardener material at the weight ratio 1:10 were used and placed on charge coupled device (CCD) as 2D grating. Afterwards, the sample was placed on vacuum chamber, and in order to dry and stabilize the pattern onto the PDMS, it was placed on heater for different times and temperatures. Now, we have perforated PDMS substrate as the first sample which must be coated with STO. As mentioned in the previous section, to investigate the surface lattice resonance of gold layer, we must prepare a second sample with bottom gold deposited layer. For this purpose, in the second sample, we coated 35 nm of gold layer by sputtering machine onto the perforated PDMS substrate before main STO coating Deposition. Finally, two produced perforated substrates were put on vacuum chamber (2×10^{-6} mbar (to be coated with STO with thickness of approximately 50 nm. The main laser source was set to the third harmonic of Nd:YAG laser with 355 nm which was focused on a target rotating at a frequency of 3 Hz at a distance of about 2 cm from the substrate. Typical laser parameters applied for deposition were as follows: pulse frequency of 10 Hz and laser fluence of 3 J/cm^2. Figure 2a illustrates the scanning electron microscopy image of the 2D perforated grating as the main substrate, with the surface area set to 5 mm^2.

The degradation rate of rhodamine-B which is obtained usually by comparing the initial and final (after photocatalysis) concentrations of the solution in the experimental setup has been shown in Fig. 2(b and c). In terms of Beer's law, this degradation percentage can be calculated using the maximum absorption value of the initial and final concentrations as [28]:

$$Deg. = \frac{C_0 - C}{C_0}\% = \frac{A_0 - A}{A_0}\%$$

1

Where, A_0 and A represent the absorption before and after the photocatalysis process respectively. The test was done after three hours by receiving UV-Vis spectrum.

Rhodamine-B of 1 ppm was prepared by adding 0.1 mg of rhodamine-B powder in 100 ml of distilled water, after which 10 ml of it was used for the test. NaOH solution was used to adjust the corresponding pH levels to 8 and 10 respectively, and HCl solution was employed to adjust the pH levels to 6, 4, and 2 respectively. The samples were slowly embedded onto the bottom of a quartz test tube facing the visible lamp source (Fig. 2b and c) (Bridgelux, 168 LED lamp of 3.2 V, 350 mA, λ > 390 nm), after which 10 ml of 1 ppm of rhodamine-B (Merck) was poured in the test tube. The visible light source cabinet and the air pump (HAILA ACO-5505) were turned on simultaneously (Fig. 2c). The degradation of rhodamine-B rate was calculated from the maximum absorption value of the UV-Visible spectrum using a spectrophotometer (Analytikjena, Specord − S600).

The application of the aquarium air pump during the photocatalytic test is very important for providing dissolved oxygen during the photocatalytic degradation. Dissolved oxygen can make the recombination process on SrTiO$_3$ difficult, causing maintenance of the electroneutrality of the SrTiO$_3$ particles [29].

In addition, two samples must be examined for chemical stoichiometry after laser deposition recorded by electron diffracted spectroscopy (EDX) as shown in Fig. 2 (d) and (e) for plasmonic and all dielectric ones respectively.

Finally, to gain a deeper insight into the new structures and the effect of perforated surface on the energy gap as well as degradation percentage, the effect of energy band structure of catalysts onto the photocatalytic property has been investigated via Kubelka−Munk function for direct and indirect band gaps of the samples [30][31].

Results And Discussion

Ultraviolet visible spectroscopy of catalysts is shown in Fig. 3a revealing the optical absorption spectra of $SrTiO_3$, $Au-SrTiO_3$, with perforated structures. It has been demonstrated that energy band and band position could affect the photocatalytic performance of photocatalysts [30]. The direct and indirect band gaps (Eg) have been calculated with $(\alpha h v)^{1/2}$ versus Energy (hv). The direct and indirect bandgaps have been obtained for perforated $SrTiO_3$ and $Au-SrTiO_3$ samples as shown in Fig. 3b, c.

By the aid of this fact that we have straight dependency between surface patterning and thus photonic bad gap and light localization in nanostructures, we simulate our perforated sample as $PDMS/SrTiO_3$ in lumerical. software. As shown in Fig. 3(d) for three first modes, we have light localization in the main unit cell due to dipole coupling.

After 3 hours and at pH10, the maximum photodegradation was achieved (16% for $PDMS\backslash Au-SrTiO_3$, and 14% for $PDMS\backslash SrTiO_3$ sample). The degradation ability of $PDMS\backslash SrTiO_3$ sample is related to the effect of the 2D nanograting substrate which may generate an intense electric field that give an additional energy to $SrTiO_3$ to make electron hall pair and start the photocatalytic activity

For $PDMS\backslash Au- SrTiO_3$, the combination of $SrTiO_3$ with a plasmonic metal leads to more effective photocatalysis efficiency. Au nanolayer can serve as charge sink, which accumulates the hot carriers, electrons or holes, in the combined $Au-SrTiO_3$ photocatalysts; thus the charge transfer and electron−hole separation will increase to enhance photocatalytic activity. $Au-SrTiO_3$ composites include charge transfer between Au and $SrTiO_3$, which highly affects the overall efficiency and is dominated basically by the Schottky barrier in the metal−semiconductor interface.

The effect of pH on RhB degradation on the degradation of the two samples was investigated within the range of 2−10. In general, the minimum value of degradation for the two samples was seen at the low values of pH (pH2, 4), where the maximum value was observed at the maximum value (pH10). The reason of this degradation is that RhB molecules at pH2 and pH4 are in the cationic form (RhB+), where the point of zero charge (PZC) of $SrTiO_3$ is 9.33 [32], and under this point $SrTiO_3$ surface is positively charged. Thus, under acidic conditions, the repulsion between RhB and $SrTiO_3$ is maximum, and the degradation will definitely be minimum. At pH7, $PDMS\backslash SrTiO_3$ degradation is slightly more than

PDMS\SrTiO$_3$-Au, which may be related to the Au positive charge causing more repulsion force with RhB at pH7 than PDMS-SrTiO$_3$. However, in an alkaline medium (pH > 7), RhB becomes deprotonated, and therefore zwitterion is formed. Hence, the electrostatic repulsion force between RhB and SrTiO$_3$ diminishes causing higher degradation of RhB. At pH > 9.3, the surface of SrTiO$_3$ is negatively charged, and the adsorption of RhB occurs more easily due to the electrostatic attraction. Since the molecules of RhB were in the zwitterionic form in the alkaline conditions, a certain part of the molecule was attracted by the catalyst surface, thus the degradation increased. In addition, in the more alkaline solution, −OH would generate more easily by oxidizing more hydroxide ions on the SrTiO$_3$ surface, thus logically enhancing the efficiency of the photocatalytic process.

Conclusions

We prepared a new plasmonic photocatalyst by depositing Au thin film on PDMS 2-dimensional grating, after which we deposited a SrTiO$_3$ thin film on Au. This was the first time a plasmonic photocatalyst like this had has been prepared. The photocatalysis activity was tested over 1 ppm rhodamine-B dye with different values of pH, using a visible light source and aquarium air pump. For PDMS\Au−SrTiO$_3$, we achieved the maximum degradation rate (16%) at pH10, where it was 14% for PDMS\SrTiO$_3$. We attributed the photocatalytic activity of the samples to the effect of the 2D nanograting on SrTiO$_3$, and to the plasmonic effect of the Au layer which can serve as a charge sink, accumulating the hot carriers, and exhibiting localized surface plasmon resonance. In addition, compositing Au−SrTiO$_3$ involved charge transfer between Au and SrTiO$_3$, which highly affects the overall efficiency by forming the Schottky barrier in the metal-semiconductor interface. Finally, for the first time we get an efficient photocatalyst, 16%, from low dimension and little area of SrTiO$_3$ sample in the visible spectrum.

Declarations

Conflict of interest:

The authors declare that they have no conflict of interest.

References

[1] C. Liao, W. Huang, and J. Wu, "Hydrogen production from semiconductor-based photocatalysis via water splitting," *Catalysts*, vol. 2, no. 4, pp. 490−516, 2012.

[2] Y. Allssa, SM Hamidi, A. Shahnazi, M. Nabid, One dimensional efficient photocatalyst based on plasmonic grating, *Opt. Quantum electronics*, 53:355, 2021.

[3] M. A. Fox and M. T. Dulay, "Heterogeneous photocatalysis," *Chem. Rev.*, vol. 93, no. 1, pp. 341−357, 1993.

[4] J. Schneider, M. Matsuoka, M. Takeuchi, J. Zhang, Y. Horiuchi, M. Anpo, and W. Bahnemann, "Understanding TiO2 photocatalysis: mechanisms and materials," Chem. Rev., vol. 114, no. 19, pp. 9919–9986, 2014.

[5] L. Sang, Y. Zhao, and C. Burda, "TiO_2 nanoparticles as functional building blocks," *Chem. Rev.*, vol. 114, no. 19, pp. 9283–9318, 2014.

[6] S. Konstas, I. Konstantinou, D. Petrakis, and T. Albanis, "Development of $SrTiO_3$ photocatalysts with visible light response using amino acids as dopant sources for the degradation of organic pollutants in aqueous systems," *Catalysts*, vol. 8, no. 11, p. 528, 2018.

[7] J. Shen, S. Wang, D. Wang, X. Shi, J. Zhang, F. Han, H. Li, "Composite Sr2 TiO4/SrTiO3 (La, Cr) heterojunction based photocatalyst for hydrogen production under visible light irradiation," J. Mater. Chem. A, vol. 1, no. 27, pp. 7905–7912, 2013.

[8] T. Alammar, I. Hamm, M. Wark, and A.-V. Mudring, "Low-temperature route to metal titanate perovskite nanoparticles for photocatalytic applications," *Appl. Catal. B Environ.*, vol. 178, pp. 20–28, 2015.

[9] K. Van Benthem, C. Elsässer, and R. H. French, "Bulk electronic structure of $SrTiO_3$: Experiment and theory," *J. Appl. Phys.*, vol. 90, no. 12, pp. 6156–6164, 2001.

[10] Y. Yamada and Y. Kanemitsu, "Band-to-band photoluminescence in $SrTiO_3$," *Phys. Rev. B*, vol. 82, no. 12, p. 121103, 2010.

[11] Z. Jiang, T. Xiao, V. áL Kuznetsov, and P. áP Edwards, "Turning carbon dioxide into fuel," *Philos. Trans. R. Soc. A Math. Phys. Eng. Sci.*, vol. 368, no. 1923, pp. 3343–3364, 2010.

[12] R. Konta, T. Ishii, H. Kato, and A. Kudo, "Photocatalytic activities of noble metal ion doped $SrTiO_3$ under visible light irradiation," *J. Phys. Chem. B*, vol. 108, no. 26, pp. 8992–8995, 2004.

[13] T. Puangpetch, S. Chavadej, and T. Sreethawong, "Hydrogen production over Au-loaded mesoporous-assembled $SrTiO_3$ nanocrystal photocatalyst: effects of molecular structure and chemical properties of hole scavengers," *Energy Convers. Manag.*, vol. 52, no. 5, pp. 2256–2261, 2011.

[14] T. Xian, L. Di, X. Sun, J. Ma, Y. Zhou, and X. Wei, "Photocatalytic degradation of dyes over Au decorated $SrTiO_3$ nanoparticles under simulated sunlight and visible light irradiation," *J. Ceram. Soc. Japan*, vol. 126, no. 5, pp. 354–359, 2018.

[15] L. Ma, T. Sun, H. Cai, Z.-Q. Zhou, J. Sun, and M. Lu, "Enhancing photocatalysis in $SrTiO_3$ by using Ag nanoparticles: A two-step excitation model for surface plasmon-enhanced photocatalysis," *J. Chem. Phys.*, vol. 143, no. 8, p. 84706, 2015.

[16] X. Ma, Y. Dai, M. Li, and B. Huang, "Oxygen vacancies at the Au/SrTiO$_3$ (001) interface: stabilities, electronic properties and effect on photocatalysis," *Phys. Chem. Chem. Phys.*, vol. 19, no. 1, pp. 774–781, 2017.

[17] D. Saadetnejad and R. Yıldırım, "Photocatalytic hydrogen production by water splitting over Au/Al-SrTiO$_3$," *Int. J. Hydrogen Energy*, vol. 43, no. 2, pp. 1116–1122, 2018.

[18] K. Wahab, T. Odedairo, J. Labis, M. Hedhili, A. Delavar, and H. Idriss, "Comparing Pt/SrTiO$_3$ to Rh/SrTiO$_3$ for hydrogen photocatalytic production from ethanol," *Appl. Petrochemical Res.*, vol. 3, no. 3, pp. 83–89, 2013.

[19] Q. Zhang, Y. Huang, L. Xu, J. Cao, W. Ho, and S. C. Lee, "Visible-light-active plasmonic Ag−SrTiO$_3$ nanocomposites for the degradation of NO in air with high selectivity," *ACS Appl. Mater. Interfaces*, vol. 8, no. 6, pp. 4165–4174, 2016.

[20] Y. Fan, Y. Liu, H. Cui, W. Wang, Q. Shang, X. Shi, G. Cui, and B. Tang, "Photocatalytic Overall Water Splitting by SrTiO$_3$ with Surface Oxygen Vacancies," *Nanomaterials*, vol. 10, no. 12, p. 2572, 2020.

[21] N. Zhou, V. López-Puente, Q. Wang, L. Polavarapu, I. Pastoriza-Santos, and Q.-H. Xu, "Plasmon-enhanced light harvesting: applications in enhanced photocatalysis, photodynamic therapy and photovoltaics," *Rsc Adv.*, vol. 5, no. 37, pp. 29076–29097, 2015.

[22] P. Wang, B. Huang, Y. Dai, and M.-H. Whangbo, "Plasmonic photocatalysts: harvesting visible light with noble metal nanoparticles," *Phys. Chem. Chem. Phys.*, vol. 14, no. 28, pp. 9813–9825, 2012.

[23] P. Zhang, T. Wang, and J. Gong, "Mechanistic understanding of the plasmonic enhancement for solar water splitting," *Adv. Mater.*, vol. 27, no. 36, pp. 5328–5342, 2015.

[24] M. Valenti, M. P. Jonsson, G. Biskos, A. Schmidt-Ott, and W. A. Smith, "Plasmonic nanoparticle-semiconductor composites for efficient solar water splitting," *J. Mater. Chem. A*, vol. 4, no. 46, pp. 17891–17912, 2016.

[25] R. Khan, W. Chuan, A. Yousuf, K. Chowdhury, and K. Cheng, "Schottky barrier and surface plasmonic resonance phenomena towards the photocatalytic reaction: study of their mechanisms to enhance photocatalytic activity," *Catal. Sci. Technol.*, vol. 5, no. 5, pp. 2522–2531, 2015.

[26] X. Zhang, Y. L. Chen, R.-S. Liu, and D. P. Tsai, "Plasmonic photocatalysis," *Reports Prog. Phys.*, vol. 76, no. 4, p. 46401, 2013.

[27] H. Liu, T. Wang, H. Zhang, G. Liu, P. Li, L. Liu, D. Hao, J. Ren, K. Chang, X. Meng, H. Wangc and J. Ye, "Room-temperature driven and visible light enhanced dehydrogenation reactions catalysed by basic Au/SrTiO$_3$," J. Mater. Chem. A, vol. 4, no. 5, pp. 1941–1946, 2016.

[28] E. T. Soares, M. A. Lansarin, and C. C. Moro, "A study of process variables for the photocatalytic degradation of rhodamine B," *Brazilian J. Chem. Eng.*, vol. 24, no. 1, pp. 29–36, 2007.

[29] M. Boroski, C. Rodrigues, C. Garcia, C. Sampaio, J. Nozaki, and N. Hioka, "Combined electrocoagulation and TiO_2 photoassisted treatment applied to wastewater effluents from pharmaceutical and cosmetic industries," *J. Hazard. Mater.*, vol. 162, no. 1, pp. 448–454, 2009.

[30] J. Xie, Y. He, X. Li, M. Duan, J. Tang, Y. Wang, M. Chamas and H. Wang, "Adjustable band position of strontium titanate by doping-free solvents effect and its correlation with photodegradation performance" J. Mater. Sci. Mater. Electron., vol. 28, no. 20, pp. 14981–14987, 2017.

[31] J. Xie, C. Yang, Y. He, and H. Wang, "Effect of pH on the phase transformation of strontium titanium materials and their photocatalytic property," *J. Mater. Sci. Mater. Electron.*, vol. 29, no. 22, pp. 19344–19352, 2018.

[32] S. Konstas, I. Konstantinou, D. Petrakis, and T. Albanis, "Synthesis, characterization of g-C3N4/SrTiO3 heterojunctions and photocatalytic activity for organic pollutants degradation," *Catalysts*, vol. 8, no. 11, p. 554, 2018.
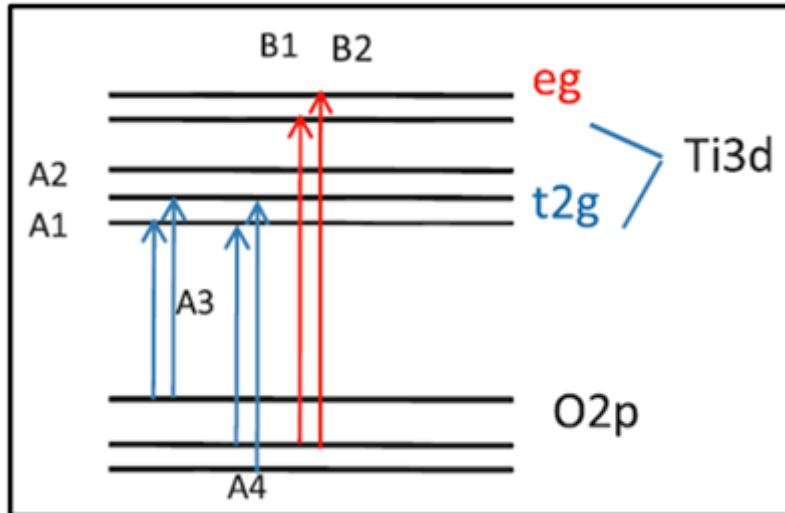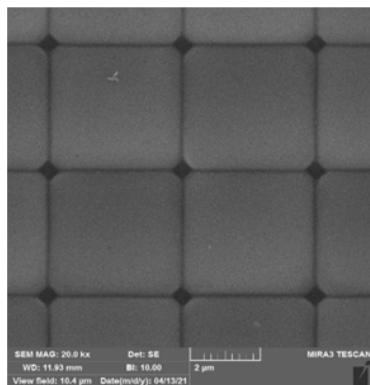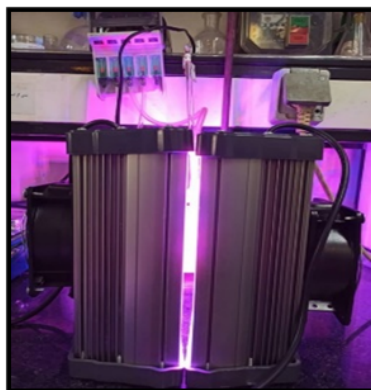
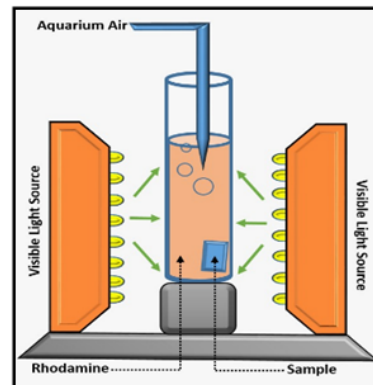# Figures

Figure 1

the electronic transitions between O2p and Ti3d levels [9]
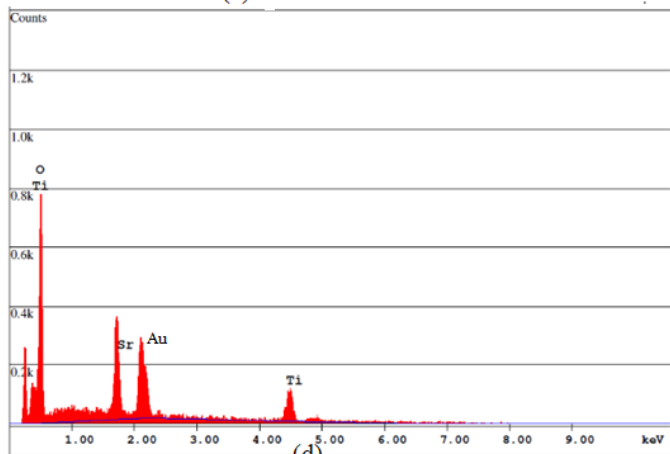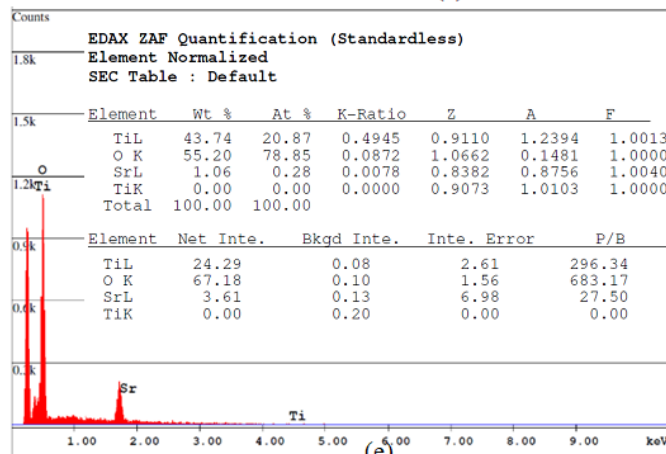
(a)   (b)   (c)

(d)   (e)

Figure 2

a) SEM image of the sample; b) photocatalysis setup, c) setup scheme in whole with contents;and EDX result of the samples: d) Au-SrTiO3; e) SrTiO3
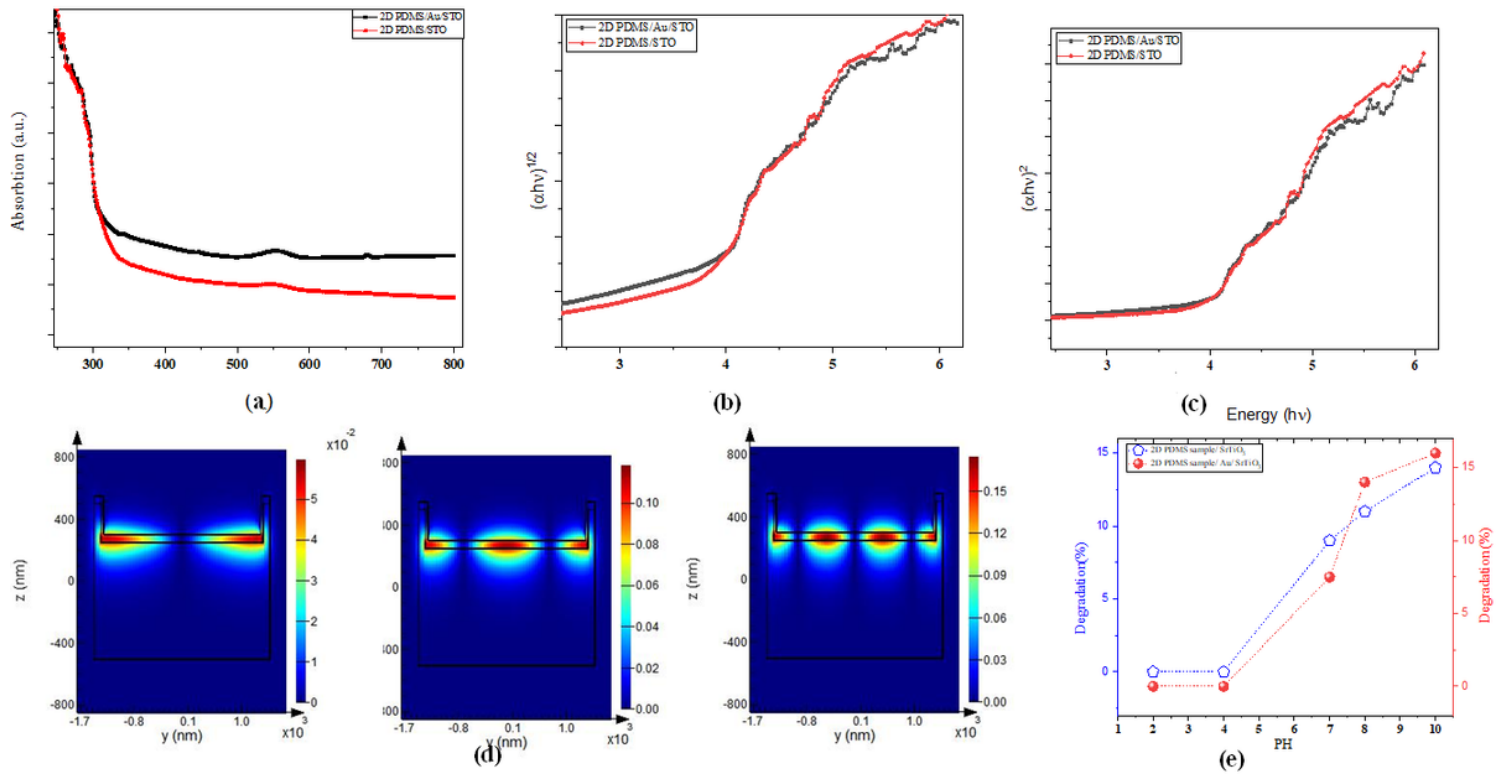
Figure 3

a) Absorbance spectra b) Tauc plot for energy gap (direct); c) energy gap (indirect); Electric field distribution of the first three modes of 2D PDMS sample SrTiO3 for: d) m=1, m=2 and m=3; e) Photocatalytic degradation of RhB with different pH for 2D PDMS\ SrTiO3 and PDMS\ Au − SrTiO3